

## Universality of (2+1)-dimensional restricted solid-on-solid models

Kelling, J.; Ódor, G.; Gemming, S.;

Originally published:

June 2016

**Physical Review E 94(2016)2, 022107**

DOI: <https://doi.org/10.1103/PhysRevE.94.022107>

Perma-Link to Publication Repository of HZDR:

<https://www.hzdr.de/publications/Publ-23645>

Release of the secondary publication  
on the basis of the German Copyright Law § 38 Section 4.

# Universality of 2+1 dimensional RSOS models

Jeffrey Kelling (2,3) Géza Ódor (1) and Sibylle Gemming (3,4)

(1) *Institute of Technical Physics and Materials Science,  
Centre for Energy Research of the Hungarian Academy of Sciences  
P.O.Box 49, H-1525 Budapest, Hungary*

(2) *Department of Information Services and Computing,  
Helmholtz-Zentrum Dresden-Rossendorf  
P.O.Box 51 01 19, 01314 Dresden, Germany*

(3) *Institute of Ion Beam Physics and Materials Research  
Helmholtz-Zentrum Dresden-Rossendorf*

*P.O.Box 51 01 19, 01314 Dresden, Germany*

(4) *Institute of Physics, TU Chemnitz  
09107 Chemnitz, Germany*

Extensive dynamical simulations of Restricted Solid on Solid models in  $D = 2 + 1$  dimensions have been done using parallel multisurface algorithms implemented on graphics cards. Numerical evidence is presented that these models exhibit Kardar–Parisi–Zhang surface growth scaling, irrespective of the step heights  $N$ . We show that by increasing  $N$  the corrections to scaling increase, thus smaller step sized models describe better the asymptotic, long wave scaling behavior.

PACS numbers: 05.70.Ln, 05.70.Np, 82.20.Wt

## I. INTRODUCTION

The Kardar–Parisi–Zhang (KPZ) equation [1] describes the evolution of a fundamental, non-equilibrium surface growth model by a Langevin equation

$$\partial_t h(\mathbf{x}, t) = \sigma \nabla^2 h(\mathbf{x}, t) + \lambda (\nabla h(\mathbf{x}, t))^2 + \eta(\mathbf{x}, t). \quad (1)$$

The scalar field  $h(\mathbf{x}, t)$  is the height, progressing in the  $D$  dimensional space relative to its mean position, that moves linearly with time  $t$ . A smoothing surface tension is represented by the coefficient  $\sigma$ , which competes a curvature-driven propagation, described by the nonlinear coefficient  $\lambda$  and a zero-average Gaussian stochastic noise. This noise field exhibits the variance  $\langle \eta(\mathbf{x}, t) \eta(\mathbf{x}', t') \rangle = 2\Gamma \delta^D(\mathbf{x} - \mathbf{x}') (t - t')$ , with an amplitude, related to the temperature in the equilibrium system, and  $\langle \rangle$  denotes a distribution average. Besides describing the dynamics of simple growth processes [2] KPZ was inspired in part by the stochastic Burgers equation [3] and is applicable for randomly stirred fluids [4], for directed polymers in random media [5] for dissipative transport [6, 7] and for the magnetic flux lines in superconductors [8].

Discretized versions have been studied a lot in the past decades [9–11]. The morphology of a surface of linear size  $L$  can be described by the squared interface width

$$W^2(L, t) = \frac{1}{L^2} \sum_{i,j}^L h_{i,j}^2(t) - \left( \frac{1}{L} \sum_{i,j}^L h_{i,j}(t) \right)^2. \quad (2)$$

In the absence of any characteristic length simple growth processes are expected to be scale-invariant

$$W(L, t) \propto L^\alpha f(t/L^z), \quad (3)$$

with the universal scaling function  $f(u)$

$$f(u) \propto \begin{cases} u^\beta & \text{if } u \ll 1 \\ \text{const.} & \text{if } u \gg 1 \end{cases} \quad (4)$$

Here  $\alpha$  is the roughness exponent in the stationary regime, when the correlation length has exceeded  $L$  and  $\beta$  is the growth exponent, describing the intermediate time behavior. The dynamical exponent  $z$  can be expressed as the ratio of the growth exponents

$$z = \alpha/\beta \quad (5)$$

and due to the Galilean invariance the  $\alpha + z = 2$  relation holds as well.

While in  $D = 1 + 1$  exact solutions are known, due to the Galilean symmetry [4] and an incidental fluctuation-dissipation symmetry [12], in higher dimensions KPZ has been investigated by various analytical [13–18] and numerical methods [19–22], still debated issues remain. For example, there is a controversy on the surface growth exponents of the  $D = 2 + 1$  KPZ, obtained by recent simulations [2, 23, 24] and a field theoretical study [25]. Assuming that the height correlations do not exhibit multi-scaling and satisfy an operator product expansion Ref. [25] concluded that growth exponents are rational numbers in two and three dimensions [25]. This was in accordance with some earlier Restricted Solid-on-Solid (RSOS) model simulation results [26, 27]. Recent high precision simulations [23, 24, 28–30] all excluded this and concluded  $\alpha = 0.393(4)$  [23, 24, 30] and  $\beta = 0.2414(15)$  [23]. RSOS models are defined by deposition at random sites if the local height difference satisfies

$$|h(\mathbf{x}, t) - h(\mathbf{x}', t)| \leq N. \quad (6)$$

Very recently Kim [31] investigated RSOS models with maximum step sizes  $N = 1, 2, \dots, 7$ . As he increased  $N$  the

roughness exponent  $\alpha$  seemed to converge to  $4/10$  and the growth exponent  $\beta$  to  $1/4$  in agreement with [25–27]. This issue is important, because one may speculate that discretized simulations cannot describe the local singularities of continuum models, i.e. finite slopes may cause corrections, responsible for the longstanding debate between field theory and discrete model simulations.

In this paper we show that the converse is true. By performing very careful corrections-to-scaling analysis on the model of Ref. [31] we show that even in case of  $N > 1$  the rational numbers of [25–27] can be excluded in the  $L \rightarrow \infty$  limit. Local slopes analysis shows, that the  $N = 1$  case has the smallest corrections and describes the KPZ universality scaling the best. For  $N > 1$  corrections corresponding shorter wavelengths are introduced. Our findings are in full agreement with the scaling results obtained for ballistic growth models [24, 32, 33].

## II. MODELS AND SIMULATION ALGORITHMS

In order to enable long time surface growth simulations of large systems, a multisurface-like parallel implementation of the RSOS model has been implemented for graphics processing units (GPUs). Two parallelization approaches have been combined as follows:

Since GPUs feature a number of vector processors, multiples of 128 realizations of the model were simulated simultaneously. This creates a data-parallel workload, which can straightforwardly be vectorized. Each single instruction multiple thread (SIMT) unit of the GPU updates 128 realizations, in which the sequence of randomly selected coordinates for update is the same. This correlation was broken by updating only half of the selected lattice sites in each attempt. If more realizations were simulated, different sets of 128 realizations evolved completely independently.

In order to handle large systems effectively a domain decomposition (DD) was also used to distribute the work of realizations among multiple SIMT elements. A double-tiling scheme was applied by splitting up the simulation cells into tiles, spitted further into two sub-tiles along each spatial direction [34]. In the present two-dimensional problem this yields  $2^d = 4$  sets of sub-tiles, each of which can be updated by multiple independent workers. After each lattice sweep the origin of the DD was moved randomly to eliminate correlations. Implementation details will be published elsewhere [35].

Roughening of  $2 + 1$ -dimensional RSOS surfaces was studied for restriction parameters  $N = 1, 3, 5, 7$ , by starting from flat initial conditions. To obtain estimates for the exponent  $\beta$ , the growth of surfaces was followed up to  $t = 10^5$  Monte-Carlo steps (MCS), which is well before the correlation length approaches the system sizes:  $L = 4096, 8192$  and  $9605$  studied here (throughout this paper the time is measured in MCS). The largest system size was bounded by memory constraints, filling up 12 GB of the NVIDIA K40 GPU, and leaving some memory for

the random number generator (RNG) states. The results were averaged over  $n = 768, 128$  and  $128$  realizations, respectively, where the latter two correspond to only one multisurface run.

The exponent  $\alpha$  was determined by a finite-size scaling analysis of the saturation roughness of system sizes between  $L = 64$  and  $L = 512$ . To keep the noise amplitude constant we used domain sizes of  $8 \times 8$  lattice sites. We determined the interface width by averaging over  $W(L, t)$  for times  $t \geq t_{\text{start}}$  and for all samples. We checked whether the averaged values belong to the steady state:  $t > t_{\text{steady}^*}$  by varying  $t_{\text{start}}$ , the onset times of the measurements. We estimated  $t_{\text{steady}^*}$  via the relation

$$a_N \cdot L^\alpha = b_N \cdot t_{\text{steady}^*}^\beta, \quad (7)$$

using the parameters  $a_N$  and  $b_N$ , deduced from fitting in small systems.

In order to estimate the asymptotic values of  $\alpha$  and  $\beta$  for  $L \rightarrow \infty$  and  $t \rightarrow \infty$ , respectively, a local slope analysis of the scaling laws were performed [36]. We calculated the effective exponents

$$\alpha_{\text{eff}} \left( \frac{L - L/2}{2} \right) = \frac{\ln W(L, t \rightarrow \infty) - \ln W(L/2, t \rightarrow \infty)}{\ln(L) - \ln(L/2)} \quad (8)$$

$$\beta_{\text{eff}} \left( \frac{t_i - t_{i/2}}{2} \right) = \frac{\ln W(L \rightarrow \infty, t_i) - \ln W(L \rightarrow \infty, t_{i/2})}{\ln(t_i) - \ln(t_{i/2})}. \quad (9)$$

In our studies the simulation time between two measurements is increased exponentially

$$t_{i+1} = (t_i + 10)e^m, \quad (10)$$

using  $m = 0.01$  and  $t_0 = 0$ , while statistical uncertainties are provided as  $1\sigma$ -standard errors, defined as  $\Delta_{1\sigma} x = \sqrt{\langle x^2 \rangle - \langle x \rangle^2 / (N - 1)}$ .

## III. SURFACE GROWTH RESULTS

### A. The Growth Regime

The growth of the surface roughness follows apparently the same, clear, power-law for all considered  $N$  (Fig. 1, top). The local slope plots (Fig. 1, down), using (9), show an effective growth exponent  $\beta_{\text{eff}} \approx 0.25$  for  $N = 5, 7$  for  $t \leq 1000$  MCS ( $t^{-1/4} \approx 0.18$ ), in agreement with Kim's results [31]. Later, the effective growth exponent decreases for all  $N > 1$ , followed over two orders of magnitude in time 1.

Expecting independence of  $\beta$  from  $N$ , it follows that the asymptotic estimates  $\beta_N$  should be the same. By assuming power-law corrections to the asymptotic scaling  $W(L \rightarrow \infty, t) \propto t^\beta(1 + t^{-x})$ , we obtained a minimal variance of the  $\beta_{N>1}$  estimates in case of  $x \simeq 0.25$ . Therefore, we plotted our  $\beta_{\text{eff}}$  results on the  $\sim 1/\sqrt[4]{t}$  scales, which

makes the tails of the curves straight in the  $N \rightarrow \infty$  limit. Logarithmic corrections to scaling were also tested, but they did not improve the extrapolations.

Table I lists the obtained estimates for  $\beta$  for the considered system sizes. Results for different  $N > 1$  are practically identical and are thus averaged to give a common value. The case  $N = 1$  is listed separately, due to the different corrections to scaling. For  $N = 1$ ,  $\beta_{\text{eff}}$  can be best extrapolated by a power-law fit with  $x = 0.90(2)$ . This is in a good agreement with the results of [37], where  $x \simeq 0.96 \simeq 4\beta$  is reported, based on the KPZ ansatz hypothesis. This motivated us testing more general scaling forms, with correction exponents multiple of  $x = \beta$ . When we combined the effective exponent forms of  $N = 1$  and  $N > 1$

$$\beta_{\text{eff}}(1/t) = \beta + a_1/t^{4\beta} + a_2/t^\beta, \quad (11)$$

with free parameters  $a_i$ , fitting for  $t \geq 148$  MCS resulted in good agreement for most of the growth region. This is shown for  $L = 8192$  by the dashed lines in Fig. 1, bottom panel. From these extrapolations we obtained the estimates:  $\beta_{N>1} = 0.2395(5)$  and  $\beta_1 = 0.2415(5)$ .

As we can observe in Fig. 1, the effective exponents suffer from stronger corrections for  $N > 1$ , than in the  $N = 1$  case. Furthermore, our data suggest a possible oscillating convergence of  $\beta_{\text{eff}}$  for  $N > 1$ , as reported in simulations of the ballistic deposition model (BD) [24]. Extrapolations based on the form (11), while in good agreement within the observed region, are prone to overfitting, where they can not cover all possible corrections. The values for  $\beta_{N>1}$  are thus underestimated, if the effective exponents do indeed show oscillating convergence.

The estimates show no clear dependence on system size, thus it can be safely assumed that all simulations are well within the scaling regime and do not suffer from finite-size effects. All results are within the margin of error of the octahedron model  $\beta = 0.2415(15)$  [23]. Most notably this is also the case for the estimates for  $N > 1$ . Overall, the presented data support  $\beta = 0.241(1)$ .

Since the curves in Fig. 1 correspond to the same  $L$  and sample size  $n$ , one can observe that the signal-to-noise ratio (S/N), the ratio between the interface width and the sample variance, increases with  $N$ . For  $N = 7$  this is higher by a factor of  $\sim 3.6$ , while for  $N = 3$  the S/N is about  $\sim 2.5$  bigger than that of the  $N = 1$  result. Presumably, the decrease of relative noise level is the consequence of a kind of self-averaging, since systems with larger allowed  $N$  accommodate more surface information than smaller ones. It is tempting to exploit this property by choosing larger height differences in the simulations, even if this can be implemented less efficiently.

## B. The Steady State

Direct fitting of the finite size scaling form

$$W_{\text{sat}}(L) \sim L^\alpha, \quad (12)$$

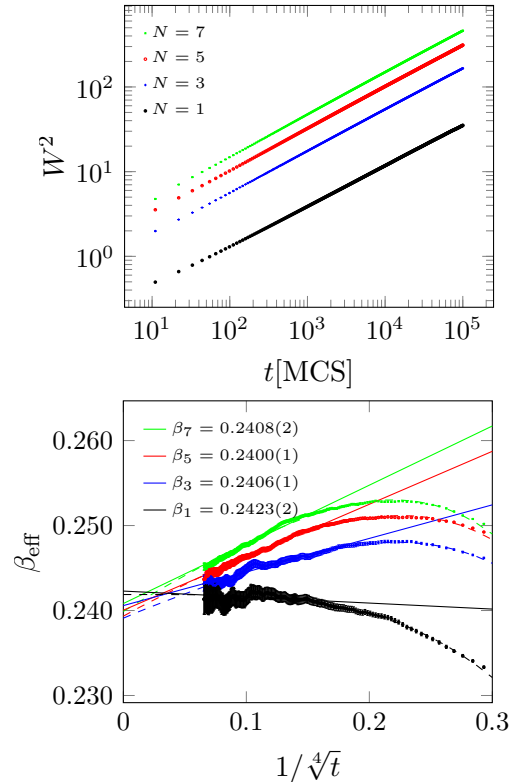


FIG. 1: Top: Squared roughness ( $W^2$ ) of surfaces of size  $V = 4096^2$  (256 realizations) in the scaling regime (error bars are smaller than symbols). Bottom: Local slope analysis of roughness scaling for size  $V = 8192^2$  (128 realizations). Straight lines are linear fits to the tail ( $t \geq 1260$  MCS), extrapolating to  $t \rightarrow \infty$ , assuming  $\sqrt[4]{t}$  corrections. Uncertainties given for  $\beta_N$  are pure fit errors. The black dashed line is the power-law extrapolation for  $N = 1$ . The dashed lines corresponding in color to the respective plots for  $N > 1$  are fits of the form (11). All PL fits were performed for  $t \geq 148$  MCS. Both figures show  $N = 1, 3, 5, 7$  (bottom to top).

TABLE I: Extrapolated  $\beta$  results for different  $N$ . Figures in the parentheses for  $N = 1$  are fit, while for  $N > 1$  case are  $1\sigma$  error estimates.

$L$	4096	8192	9605
$\beta_1$	0.2412(1)	0.2418(1)	0.2415(1)
$\beta_{N>1}$	0.2404(3)	0.2405(3)	0.2410(3)

for  $32 \leq L \leq 512$  and  $t_{\text{start}} = 50t_{\text{steady}^*}$  yields the following estimates

$$\alpha_{\text{fit}} = \begin{cases} 0.392(1) & 0.392(5) & N=1 \\ 0.401(2) & 0.400(4) & N=3 \\ 0.402(2) & 0.401(4) & N=5 \\ 0.402(2) & & N=7 \end{cases}$$

For comparison, Kim's results [31] are shown in the second column. When we decrease  $t_{\text{start}}$  our values decrease slightly, but fall inside the error margins if  $t_{\text{start}} \geq$

$2t_{\text{steady}^*}$ . So, direct fits match perfectly those of [31], obtained by sequential Monte Carlo updates.

However, if the  $L = 32$  data are excluded, our estimates become significantly lower, warning for strong corrections to scaling. This can also be seen with the help of the effective exponents in Fig. 2 calculated by (8). There is a clear tendency for  $\alpha_{\text{eff}}$  to decrease as we increase the system size for the  $N > 1$  cases. The approach to  $L \rightarrow \infty$  is nonlinear, but the number of points is insufficient for PL extrapolations to produce consistent estimates. We plotted the  $\alpha_{\text{eff}}(L)$  results on the  $1/\sqrt{L}$  scale, resulting in points that can be settled on straight lines. Linear extrapolation to asymptotically large sizes yields:

$$\alpha = \begin{cases} 0.391(1) & N = 1 \\ 0.386(1) & N > 1 \end{cases}$$

Corrections to finite-size scaling (12) in case of  $N = 1$  are small, explaining the good agreement between local slope analysis and the direct fit. The slight difference between the  $N = 1$  and  $N > 1$  results may be attributed to the fact that our data points are not deeply enough from the steady state. This might also explain the disagreement with the results of a recent study [30], which reported  $\alpha = 0.3869(4)$  for  $N = 1$ . There is a further uncertainty of the extrapolation to  $L \rightarrow \infty$ , which is not accounted for by the fit errors. With the assumption of an intrinsic width:  $W_i^2 = 0.2$  [32], the local slopes analysis shows stronger corrections to scaling, therefore we did not apply this in our study.

The observation of stronger corrections for larger  $N$ -s is consistent with a recent analysis of the BD. [24] This study found that corrections to scaling, for both  $\alpha$  and  $\beta$ , are reduced, when the BD surface is smoothed by binning of the surface positions before analysis, thereby decreasing the height differences between neighboring sites. Binning of the surface did not change the universal behavior, it only decreased non-universal corrections. The corrections produced even an oscillatory approach to the asymptotic values of the exponents. This can explain why our simple extrapolations of  $\alpha_{\text{eff}}$  (Fig. 2) and  $\beta_{\text{eff}}$  (Fig. 1) for  $N > 1$  undershoot those of  $N = 1$ .

All of our estimates up to  $N \leq 7$ , obtained by the local slope analysis, are in the range  $\alpha = 0.390(4)$ , which clearly excludes  $\alpha = 2/5$ . Plugging our  $\alpha$  and  $\beta$  results into the scaling relation (5) we get the dynamical exponent estimates  $z_{N=1} = 1.61(2)$  and  $z_{N>1} = 1.60(2)$ , respectively. The scaling law following from the Galilean invariance is satisfied with these exponents both for  $N = 1$ :  $\alpha + z = 2.01(2)$  and  $N > 1$ :  $\alpha + z = 1.99(2)$  within error margins.

We have also tested the scaling form (3) numerically by using our  $\alpha$  and  $\beta$  values. As Fig. 3 shows good data collapses can be obtained for  $N > 1$  and even a perfectly looking one for  $N = 1$ . For  $N > 1$  in the growth regime a perfect one can also be achieved assuming the values suggested by Kim and Kosterlitz [26] (Fig. 3, top). This can be understood by taking into account the corrections

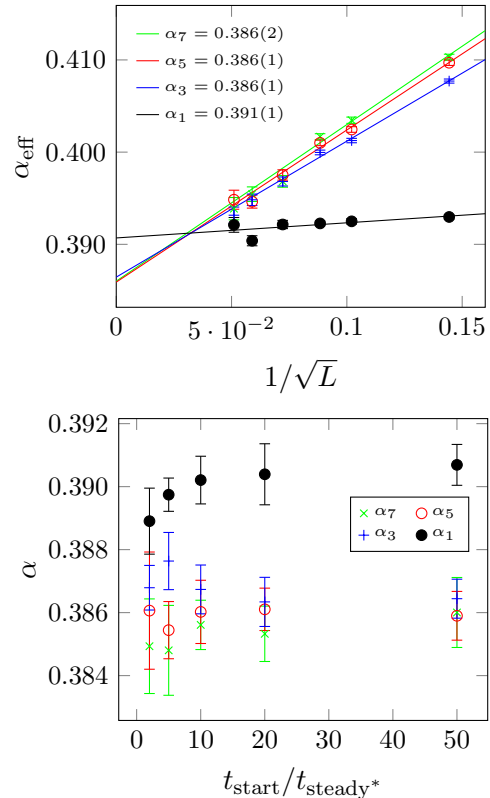


FIG. 2: Top: Local slopes of finite-size scaling analysis with  $N = 1, 3, 5, 7$ . Error bars are propagated  $1\sigma$  errors. Straight lines are linear fits to extrapolate to infinity, uncertainties given for  $\alpha_N$  are pure fit errors. Steady-state data taken for  $t > t_{\text{start}} = 50t_{\text{steady}^*}$  (see text). Bottom: Dependence of extrapolated  $\alpha$  on  $t_{\text{start}}$  is weak. Both figures: Sample sizes are at least 1024-2048 realizations and  $\geq 8192$  realizations for  $L \leq 64$ . All system sizes taken into account for finite-size scaling are listed in Fig. 3, where the considered timescales can also be read off.

to scaling we explored above. Effective exponents for early times and small systems agree with the conjecture by [26] and indeed the most strongly outlying curves in Fig. 3, top, correspond to smaller systems.

We also calculated some standard measures, the skewness

$$S = \langle (\Delta h)^3 \rangle / \langle (\Delta h)^2 \rangle^{3/2} \quad (13)$$

and the kurtosis

$$Q = \langle (\Delta h)^4 \rangle / \langle (\Delta h)^2 \rangle^2 - 3 \quad (14)$$

of our width-distributions in the steady state. The obtained values show no significant dependence on  $N$ , our best results are  $S = 1.70(1)$  and  $Q = 5.38(4)$ , in good agreement with those of [22].

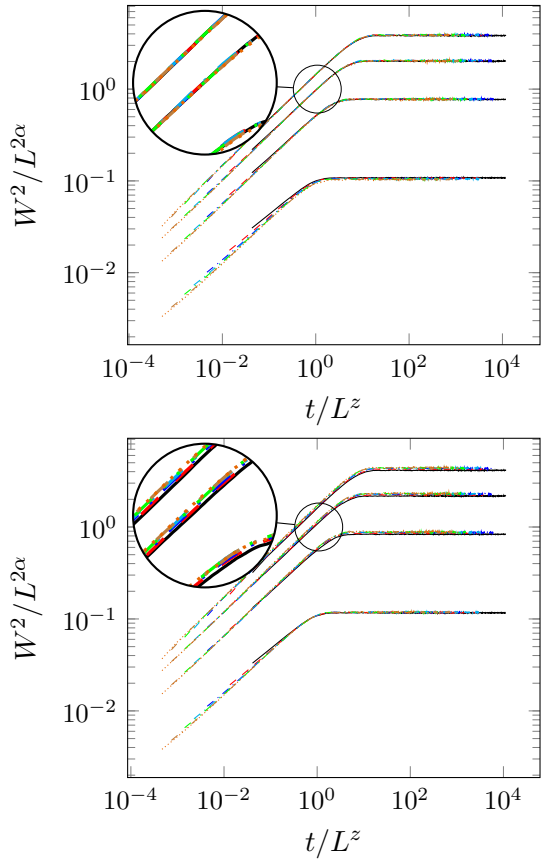


FIG. 3: Collapse of squared roughness in the steady state for  $N = 1, 3, 5, 7$  (from bottom to top). The top figure shows a perfect collapse for  $N > 1$ , using  $\alpha = 0.4$  and  $\beta = 0.25$  ( $z = \alpha/\beta = 1.6$ ). The bottom figure shows a collapse using  $\alpha = 0.389$  and  $\beta = 0.241$  ( $z \approx 1.61$ ). This looks perfect for  $N = 1$ , but not for  $N > 1$ .

### C. Consistency of Fine-Size Scaling with Respect to DD

Since we used a parallel DD in our simulations we have also checked for dependence of the results on the applied scheme. We performed additional finite-size scaling studies with domains of  $16 \times 16$  and  $6(+1) \times 10(+1)$  lattice sites. The figures in the parentheses refer to irregular tiling of the system. This is the consequence of the fact, that lattices cannot be divided into domains with a lateral size of six (or ten) sites without remainder, thus a subset of domains have larger lateral size to compensate it. This configuration results from dividing the system into multiples of  $5 \times 3$  tiles, in order to achieve optimal load balancing on NVIDIA GTX Titan Black GPUs. In both cases the smallest considered system size was  $L = 64$  to avoid unreasonable DD. Another test was done using  $3(+1) \times 5(+1)$  sized domains. These tiles turned out to be too small to give correct results, expressed by failing data collapses, thus we do not consider them in the following discussion.

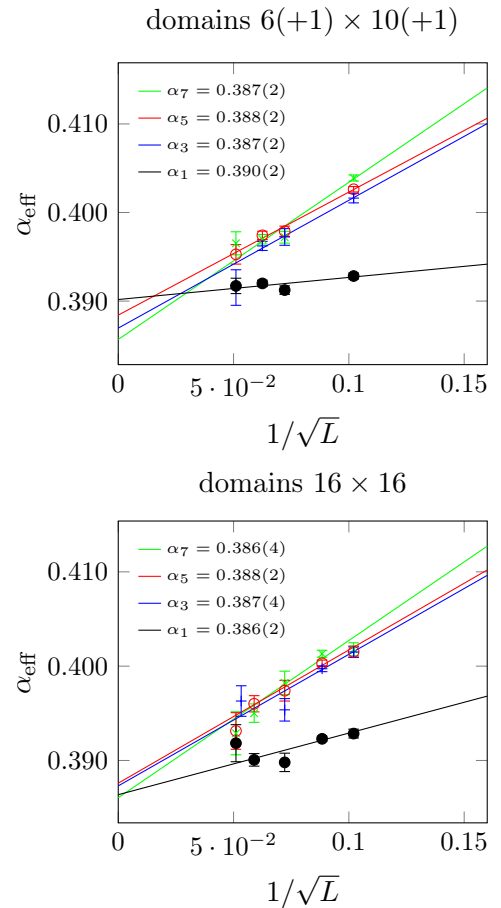


FIG. 4: Local slopes of finite-size scaling analysis for  $N = 1, 3, 5, 7$ . Error bars are propagated  $1\sigma$  errors. Straight lines are linear fits to extrapolate to infinity, uncertainties given for  $\alpha_N$  are pure fit errors. Steady-state data is taken for  $t > t_{\text{start}} = 50t_{\text{steady}^*}$  (see text). Top: DD domains containing  $6(+1) \times 10(+1)$  sites. Sample sizes are at least 512 realizations, for  $N = 5, 7$  and sizes  $L = 64$  and  $128$ ,  $n = 16384$   $n = 8192$  are used. Bottom: DD domains containing  $16 \times 16$  sites. For  $L = 512$  the sample contains 256 realizations, for other system sizes at least 512 samples are included.

The differences among the results of the considered DD configurations were not significant in the data collapses, nor in the finite-size scaling fits. The most sensitive quantity proved to be the effective roughness exponent, shown in Fig. 4. Sample sizes of this test were smaller than those of Sect. III B, making the extrapolations less reliable. Still, all estimates derived from this data are consistent with the estimate  $\alpha = 0.390(4)$ . Even the results of irregular, non-square DDs do not deviate significantly, although small systematic errors might be present.

#### IV. CONCLUSIONS

Extensive numerical simulations have been performed for  $2+1$  dimensional RSOS models with variable height difference restrictions. Careful correction to scaling analysis has provided numerical evidence, that the universal surface growth exponents agree with the most precise values known for the  $2+1$  dimensional KPZ class. These estimates:  $\alpha = 0.390(4)$  and  $\beta = 0.2415(3)$  exclude the rational values  $\alpha = 4/10$  and  $\beta = 1/4$ , conjectured by [25–27, 31]. Our results support the generalized KPZ ansatz, which takes finite time corrections into account and predicts exponents  $x$  that are multiples of  $\beta$  [37]. We found  $x = 0.90(2)$  for  $N = 1$  and  $x \simeq 0.25$  for  $N > 1$ .

We have shown that by increasing the local height differences we obtain better S/N in the simulations, but stronger corrections to scaling, which can confuse numerical analysis based on simple power-law fitting. Therefore, smaller step sized models, like the octahedron model [23] describe better the asymptotic, long wave scaling behavior of the KPZ universality class. Our conclusions for scaling-corrections are in agreement with those, obtained for ballistic growth models [24, 32]. According to our knowledge oscillating convergence of effective exponents has not yet been observed in RSOS models warning further investigations. We also provided estimates for the skewness  $S = 1.70(1)$  and the kurtosis  $Q = 5.38(4)$  of the steady state surface width distributions. Our simulations have been performed using multisurface GPU SIMT algorithms with origin moving domain decomposi-

tion. The results have been justified by varying the tile sizes. A sustained performance of  $\simeq 1.1 \times 10^{10}$  deposition attempts per second could be achieved running on a single NVIDIA GTX Titan Black GPU. This opens up the possibility for precise RSOS simulations in higher dimensions.

#### Acknowledgments:

We thank S. Alves for sending us the correction to scaling plot of exponent  $\alpha$  of the 3D ballistic growth, S. C. Ferreira and T. Halpin-Healy for useful comments. Support from the Hungarian research fund OTKA (Grant No. K109577), the Initiative and Networking Fund of the German Helmholtz Association via the W2/W3 Programm für exzellente Wissenschaftlerinnen (W2/W3-026) and the Helmholtz International Research School for Nanoelectronic Networks NanoNet (VH-KO-606) is acknowledged. We gratefully acknowledge computational resources provided by the HZDR computing center, NIIF (Budapest and Debrecen) and the Center for Information Services and High Performance Computing (ZIH) at TU Dresden (Taurus). We acknowledge support by the GCoE Dresden. J. K. thanks M. Weigel of the Applied Mathematics Research Centre at Coventry University for providing a guest position, co-funded through the Erasmus+ program via the Leonardo-Büro Sachsen.

- 
- [1] M. Kardar, G. Parisi, and Y.-C. Zhang, Phys. Rev. Lett. **56**, 889–892 (1986), URL <http://link.aps.org/doi/10.1103/PhysRevLett.56.889>.
  - [2] T. Halpin-Healy, Phys. Rev. A **42**, 711–722 (1990), URL <http://link.aps.org/doi/10.1103/PhysRevA.42.711>.
  - [3] J. M. Burgers, *The nonlinear diffusion equation : asymptotic solutions and statistical problems* (Dordrecht-Holland ; Boston : D. Reidel Pub. Co, 1974), ISBN 9027704945, first published in 1973 under title: Statistical problems connected with asymptotic solutions of the one-dimensional nonlinear diffusion equation.
  - [4] D. Forster, D. R. Nelson, and M. J. Stephen, Phys. Rev. A **16**, 732–749 (1977), URL <http://link.aps.org/doi/10.1103/PhysRevA.16.732>.
  - [5] M. Kardar, Phys. Rev. Lett. **55**, 2923–2923 (1985), URL <http://link.aps.org/doi/10.1103/PhysRevLett.55.2923>.
  - [6] H. van Beijeren, R. Kutner, and H. Spohn, Phys. Rev. Lett. **54**, 2026–2029 (1985), URL <http://link.aps.org/doi/10.1103/PhysRevLett.54.2026>.
  - [7] H. Janssen and B. Schmittmann, Zeitschrift für Physik B Condensed Matter **63**, 517–520 (1986), ISSN 0722-3277, URL <http://dx.doi.org/10.1007/BF01726201>.
  - [8] T. Hwa, Phys. Rev. Lett. **69**, 1552–1555 (1992), URL <http://link.aps.org/doi/10.1103/PhysRevLett.69.1552>.
  - [9] P. Meakin, P. Ramanlal, L. M. Sander, and R. C. Ball, Phys. Rev. A **34**, 5091–5103 (1986), URL <http://link.aps.org/doi/10.1103/PhysRevA.34.5091>.
  - [10] A. Barabási and H. Stanley, *Fractal Concepts in Surface Growth* (Cambridge University Press, 1995), ISBN 9780521483186, URL <https://books.google.de/books?id=W4SqcNr8PLYC>.
  - [11] J. Krug, Advances in Physics **46**, 139–282 (1997), URL <http://dx.doi.org/10.1080/00018739700101498>.
  - [12] M. Kardar, Nuclear Physics B **290**, 582–602 (1987), ISSN 0550-3213, URL <http://www.sciencedirect.com/science/article/pii/0550321387902033>.
  - [13] T. Kloss, L. Canet, and N. Wschebor, Phys. Rev. E **86**, 051124 (2012), URL <http://link.aps.org/doi/10.1103/PhysRevE.86.051124>.
  - [14] M. Schwartz and S. F. Edwards, EPL (Europhysics Letters) **20**, 301 (1992), URL <http://stacks.iop.org/0295-5075/20/i=4/a=003>.
  - [15] E. Frey and U. C. Täuber, Phys. Rev. E **50**, 1024–1045 (1994), URL <http://link.aps.org/doi/10.1103/PhysRevE.50.1024>.
  - [16] M. Lässig, Nuclear Physics B **448**, 559–574 (1995), ISSN 0550-3213, URL <http://www.sciencedirect.com/science/article/pii/055032139500268W>.
  - [17] H. C. Fogedby, Phys. Rev. Lett. **94**, 195702 (2005), URL <http://link.aps.org/doi/10.1103/PhysRevLett.94.195702>.

- 195702.
- [18] L. Canet, H. Chaté, B. Delamotte, and N. Wschebor, Phys. Rev. E **84**, 061128 (2011), URL <http://link.aps.org/doi/10.1103/PhysRevE.84.061128>.
- [19] B. M. Forrest and L.-H. Tang, Phys. Rev. Lett. **64**, 1405–1408 (1990), URL <http://link.aps.org/doi/10.1103/PhysRevLett.64.1405>.
- [20] T. Halpin-Healy, Phys. Rev. Lett. **109**, 170602 (2012), URL <http://link.aps.org/doi/10.1103/PhysRevLett.109.170602>.
- [21] E. Marinari, A. Pagnani, and G. Parisi, Journal of Physics A: Mathematical and General **33**, 8181 (2000), URL <http://stacks.iop.org/0305-4470/33/i=46/a=303>.
- [22] F. D. A. A. Reis, Phys. Rev. E **72**, 032601 (2005), URL <http://link.aps.org/doi/10.1103/PhysRevE.72.032601>.
- [23] J. Kelling and G. Ódor, Phys. Rev. E **84**, 061150 (2011), URL <http://link.aps.org/doi/10.1103/PhysRevE.84.061150>.
- [24] S. G. Alves, T. J. Oliveira, and S. C. Ferreira, Phys. Rev. E **90**, 052405 (2014), URL <http://link.aps.org/doi/10.1103/PhysRevE.90.052405>.
- [25] M. Lässig, Phys. Rev. Lett. **80**, 2366–2369 (1998), URL <http://link.aps.org/doi/10.1103/PhysRevLett.80.2366>.
- [26] J. M. Kim and J. M. Kosterlitz, Phys. Rev. Lett. **62**, 2289–2292 (1989), URL <http://link.aps.org/doi/10.1103/PhysRevLett.62.2289>.
- [27] J. M. Kim, J. M. Kosterlitz, and T. Ala-Nissila, Journal of Physics A: Mathematical and General **24**, 5569 (1991), URL <http://stacks.iop.org/0305-4470/24/i=23/a=022>.
- [28] T. Halpin-Healy, Phys. Rev. E **88**, 042118 (2013), URL <http://link.aps.org/doi/10.1103/PhysRevE.88.042118>.
- [29] S. G. Alves, T. J. Oliveira, and S. C. Ferreira, Phys. Rev. E **90**, 020103 (2014), URL <http://link.aps.org/doi/10.1103/PhysRevE.90.020103>.
- [30] A. Pagnani and G. Parisi, Phys. Rev. E **92**, 010101 (2015), URL <http://link.aps.org/doi/10.1103/PhysRevE.92.010101>.
- [31] J. M. Kim, Journal of the Korean Physical Society **67**, 1529–1532 (2015), ISSN 0374-4884, URL <http://dx.doi.org/10.3938/jkps.67.1529>.
- [32] S. G. Alves and S. C. Ferreira, ArXiv e-prints (2016), 1603.08457.
- [33] S. Alves, private communication.
- [34] J. Kelling, G. Ódor, M. F. Nagy, H. Schulz, and K. Heinig, The European Physical Journal - Special Topics **210**, 175–187 (2012), ISSN 1951-6355, URL <http://dx.doi.org/10.1140/epjst/e2012-01645-8>.
- [35] J. Kelling, M. Weigel, G. Ódor, and S. Gemming (2016), to be published.
- [36] G. Ódor, *Universality in Nonequilibrium Lattice Systems* (World Scientific, 2008).
- [37] T. J. Oliveira, S. G. Alves, and S. C. Ferreira, Phys. Rev. E **87**, 040102 (2013), URL <http://link.aps.org/doi/10.1103/PhysRevE.87.040102>.